Interference Avoidance Routing Strategy in Cognitive Radio Networks

Minh Thao Quach, Francine Krief
LaBRI, University of Bordeaux
Talence, France
Email: quach@labri.fr and krief@labri.fr

Mohamed Aymen Chalouf
IRISA, University of Rennes
Rennes, France
Email: mohamed-aymen.chalouf@irisa.fr

***Abstract*—Co-existence between legacy wireless infrastructure and a cognitive radio network has been attracting the research community. However, many challenges arise due to several difficulties, such as how to leverage current deployment for a secondary network but guarantee no interference to the primary network. This work illustrates a specific coexistence deployment in which a primary coverage reception overlaps with a cognitive transmitter's reception zone. We show that typically, a large overlap zone causes high interference; however, the interference level is lower when the node density is minor. Fuzzy logic is used to combine observed factors of the wireless environment (e.g., area overlapping and primary receiver density) to estimate interference level to primary receivers. The computed results reflect the precise impact that may occur when a cognitive radio communication is operating nearby. Interference level is retrieved by the routing engine and becomes a routing metric alternative to the hopcount metric for our routing proposal, which leverages Dynamic MANET On Demand for cognitive radio networks. In this paper, we detail the proposed routing idea, which promotes a cross-layered routing design for cognitive radio networks and incorporates observed environment information to prevent severe interference with primary networks.**

Keywords–Cognitive radio; overlap region; prediction model; fuzzy logic; interference avoidance.

I. INTRODUCTION

The objective of this paper is to define a routing strategy which avoids interference in cognitive radio networks (CRNs). This strategy is essentially based on our previous work [1]. To make the readers easy to follow, we present the reason why CRNs were introduced. Due to the limitation of fixed broadband and frequency range allocation, there is a huge need for enhancing radio resource usage using cognitive radio technologies, especially for the rural areas. The federal communications commission (FCC) has been conducting data collection and evaluating the communication needs of rural communities since 2008 in the US [2]–[4]. Expanding broadband deployment for rural areas is critical, however their full impact has not been yet realized and it would be interesting to measure this impact.

As illustrated in Figure 1 [5], CRN infrastructure can coexist with an existing primary system including the primary transmitter base station and its primary receivers. Again, evaluating the impact with this co-existing scheme should be studied since it has not been realized thoroughly. To do so, we are interested in studying the reception overlap between the secondary transmitter and primary transmitter and observing its impact on the primary receivers.

Eliminating interruptions during an operation is one of the key properties of reliable applications or services. In CRNs,

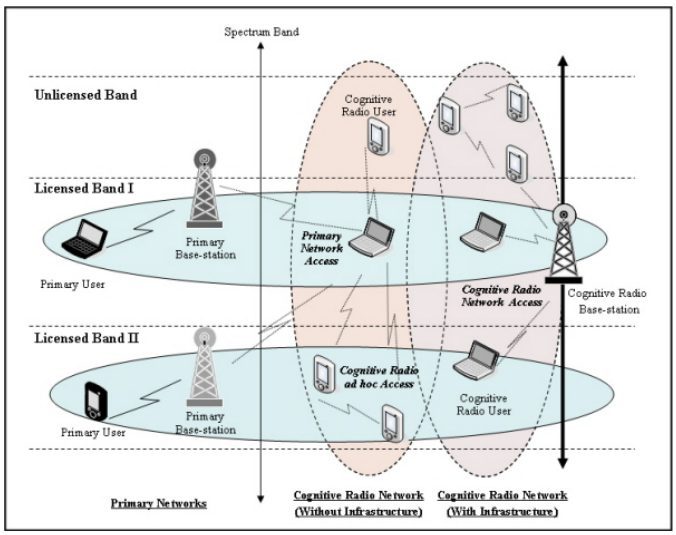

Figure 1. Cognitive radio networks reference architecture

interruptions obviously happen when the transmission of a primary radio (PR) forces cognitive radios (CRs) to vacate on the selected band. On the other hand, when an overlap exists in the coverage area between the CR and PR transmitters, the undesired interference generated by the secondary transmitters on PR communications becomes difficult to control. For this reason, it is necessary to accurately characterize this overlap and its effect on every available channel for better spectrum selection.

We define an overlap region as an area where a PR emitter's signal meets a CR emitter's signal. In case of coexistence, this area is vulnerable to the operating primary receivers within the region. When it comes to protecting PR receivers' communication, avoiding this vulnerable area is one of the options. However, since these receivers are not always operating continuously on this area, the spare spectrum within this area can be exploited and used by CR nodes. Considering the line-of-sight propagation model in rural areas, we define an overlap in CRN context as being a geometrical overlapping area between two circles that were formed by the signal of the PR and CR transmitters. As illustrated in Figure 2, the PR transmitter overlaps with two other CRs that creates two overlap regions, overlap region 1 and overlap region 2 respectively.

We rely on the position of the transmitters and their transmission ranges to identify the encountered overlap situations. Different overlapping cases have different effects on

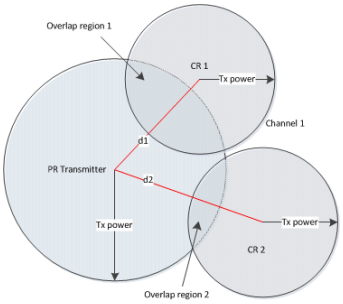

Figure 2. Overlap in cognitive radio networks definition

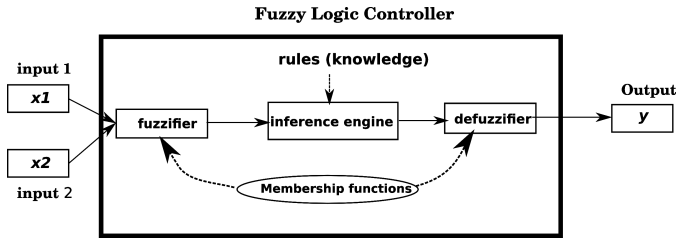

Figure 3. General fuzzy logic system

the primary receivers. Therefore, characterizing all these cases provides better vision on designing an interference-free CR communication scheme. For instance in a rural area, a CRN overlaps with TV transmission signals; the overlap area size could be variable. Assuming that a smaller overlap region leads to less impact on possible TV receivers, this CRN can operate on the area that has small overlapping area. As long as the impact on the receivers is observed, the interference can be avoided.

In a CRN, a CR node makes decisions based on its own observed information even though this knowledge may be incomplete. Fuzzy logic, however, can yield useful outputs with incomplete, approximate or vague information (e.g., low or high interference, sufficient or insufficient available radio resources). Furthermore, fuzzy logic does not require too complicated computation since the calculation is mostly based on if-then-else rules. Hence, we can use fuzzy logic in real-time cognitive radio applications for which the response time is crucial to the system performance [6]. Due to its simplicity, flexibility, and if-then-else rules composition, processing time for fuzzy logic is minor.

Fuzzy logic introduces a logic theory that was developed to generalise 'true' and 'false' values to any value between 0 and 1 [7]. It also presents the approximate knowledge, which may be difficult to express by conventional crisp methods (i.e., bivalent set theory). A fuzzy logic system with two inputs and one output is described in Figure 3. The fuzzy sets are sets of unsharp boundaries in which membership is a matter of degree (in range of 0 to 1). For instance, a fuzzy set of $weekend$ may contain half of Friday, Saturday and Sunday and a set of $weekdays$ may contain from Monday to the first half of Friday. So, Friday can exist in both sets with distinctive degrees. To identify the degree of these variables, a membership function is used to imply the related information. The membership function assigns a value in the interval $[0, 1]$ to a fuzzy variable, denoted by $\mu(weekend(day))$, where $weekend$ is a fuzzy set, and day is a fuzzy variable.

Input crisp values are fuzzified to produce appropriate linguistic values according to defined membership functions. Then, the inference engine will extract the associated outputs based on the defined rules. These outputs are fuzzified based on output membership functions. Finally, fuzzified outputs are aggregated into a single crisp value by the defuzzifier.

The output can be used to investigate how the routing layer reacts and makes the right decisions to maximise spectrum resources while avoiding interference with the primary receivers. For instance, a CR can operate within an area which has high overlap size but low number of operating primary receivers. We apply fuzzy logic to determine the overlap size and the probability of operating primary receivers (e.g., low or high).

In the literature, we did not find any explicit solution or proposal that is sufficient to protect the PR when coexistence happens. There is always a trade-off between the coexistence and interference. In our previous works [8], [9], we graphically observed and estimated how the PRs get impacted when overlap happens along with a proposal of using the stochastic model Grey and Kalman filter to predict the potential PRs that may be impacted. From these observations, we proposed a method to combine these two factors using fuzzy logic, which was detailed in [1]. We explain this again in this article so that the readers understand the proposed routing framework.

The rest of the paper is structured as follows. A literature review of routing solutions in CRN is provided in Section II. Then we briefly present the overlap calculation and the node density estimation method in Section III. The method to compose these two factors into an interference level, in which we estimate this level using fuzzy logic and a routing proposal, is in Section IV and V. Overall, we conclude our work in Section VI.

II. Related Work

Network layer plays an important role in computer network communication, essentially, routing protocol to establish a path between a sender and a receiver. Routing in a wireless network is always an interesting topic in the research community. In CRNs, the routing problem imposes a great challenge due to the dynamic spectrum access nature. If two neighboring nodes do not have a common accessible channel, or they have a common channel but do not tune to the same frequency, the communication in this case is infeasible and no route can ever be established. In CRNs, topology construction includes spectrum detection, neighbor discovery, and topology management. In some circumstances, a routing decision also depends on the required Quality of Service (QoS) from upper layer and also from the control information from the lower layers (PHY and MAC).

Due to the unique function of a CRN, intermittent link is the first challenge that any routing solution needs to tackle. To be specific, routing challenges in CRNs include spectrum awareness, quality route discovery process, and route maintenance/reparation mechanism [10]. Researchers hence have to keep in mind the fact that they will not have any pre-allocation spectrum access for the routing module, so the routing algorithm has to accommodate the change of the environment.

However, the algorithm also has to satisfy the basic network performance [11]. Nevertheless, an inter-dependence solution between route selection and spectrum management could be an appropriate approach to resolve the spectrum awareness issue [12].

Routing over the open spectrum environment is a fundamental issue, especially in dealing with multi-hop CRNs. Several routing solutions were proposed but no general routing solution exists [13]. Again, the challenge is how to ensure radio resources for cognitive transmission while guaranteeing the service for all on-going PR communications over the exploited channels on the whole path. Regarding service-wise perspective, the question is how many possible services can be provided to the end users in the secondary networks. Overall, any routing solution in CRNs should always be aware of the potentially available spectrum that may be provided by the sensing function locally or globally. Research by Cesana, Cuomo, and Ekici [10] classified two main classes of routing algorithm, full spectrum knowledge and local spectrum knowledge, which consider global and local spectrum information among CRs as the main criteria for routing algorithm classification.

Cheng et al. [14] proposed a spectrum-aware routing solution that selects a route according to the switching delay among channels and backoff delay within a channel based on the spectrum information provided. Also, research by Liu, Cai, and Shen [15], another spectrum-aware routing solution, suggested coupling spectrum sensing and spectrum sharing in multichannel for multi-hop routing. Based on the location information and channel statistic, a CR selects the relay hop and adapts its own transmission to dynamic spectrum access opportunities in its neighbor. The authors proposed a routing metric that encountered the throughput called cognitive transport throughput as the main metric for the protocol. This metric was used to capture the dynamic change from sensing information and evaluate potential gain of each relay hop. In term of spectrum-aware solutions, Zhu, Akyildiz, and Kuo [16] also built a spectrum tree based as on-demand routing solution for Cognitive Radio Ad-Hoc Networks (CRAHNs). The global sensing and sharing information were utilized to build a tree with distinguished levels of available spectrum on each band. They suggested cooperating this information from the spectrum decision and routing selection process to produce a metric and adapt an on-demand routing protocol for CRAHNs. Other on-demand routing adaptations for CRNs were also introduced in [17], [18].

Some other works that also take into account the cooperation between spectrum sensing and the routing module were introduced in [19], [20]. Xin, Xie, and Shen [19] proposed a graph-based solution that associated spectrum sensing decisions with the radio interfaces of each node in the network to assign specific spectrum opportunities to the radio interfaces, while Krishnamurthy et al. [20] modified MAC layer configurations to determine a common set of channels to facilitate communication among the nodes. The topology so is formed according to this common set of discovered channels. This solution indeed used the global spectrum knowledge to accommodate the routing algorithm. Additionally, the physical location of each node was also disclosed among the node to provide the global view of the network topology.

Once the knowledge of the surroundings is partially learned, Guan et al. [21] proposed a prediction-based middleware between the network layer and lower layers. The authors studied topology control and routing issues in Cognitive Radio MANETs (CR-MANETs) and built a middleware-like cross-layer module to provision cognition capacity to do routing for CR-MANETs. The work aimed to capture the dynamic change of topology and potentially construct an efficient and reliable topology. Indeed, the solution is the inter-dependence component as mentioned between MAC layer and routing layer, and this component incorporates sensing statistics to predict and provide information on the available duration of link to routing components. Other solutions that deal with opportunistic networks include an opportunistic access routing solution in [13], where routing metric was rendered based on demanded QoS in cooperation with the channels' access opportunities.

Location awareness is another aspect of concern in CRN routing. A geographic forwarding based Spectrum Aware Routing protocol for Cognitive ad-Hoc networks (SEARCH) is also a location awareness routing solution in [22] that joined undertaken paths to completely avoid the PR's region, while routing to protect the PR devices within this area. Similarly, Habak et al. [23] suggested location-aware routing solutions could provide better protection for PR devices from CRNs' communication. Also, a routing solution with consideration about overlapping was proposed in [24]. PR receivers protection was studied in this work as the main purpose. The routing mechanism ensured a perfect protection for PRs by selecting routes that avoid any overlap between PR and secondary radio coverage. However, the resources of the overlap region may be usable when the PR receivers are inactive or non-existent.

Even though the research community has been spending considerable resources and effort to resolve routing challenges for CRNs, there are still no routing standards that could overcome all the challenges. Routing issues encountered in CRN design can be varied. Each hop has its own different expectation of available resources (channels, frequency range, power level, interference level, etc.) and allocation time. Therefore, most of the existing solutions treat routing designs as a cross-layered problem with cooperation between a lower layer, e.g., to acquire sensing information and to render potential resources, and the routing mechanism on the network layer to establish a path among nodes.

Another perspective that attracts the research community is interference analysis in CRNs. The investigation of interference analysis takes a critical role to provide input to design various network parameters to guarantee certain performance for the primary users [25]. Many studies have been carried out in [26]–[30]. Hossain et al. [25] have studied and classified two types of interference configuration, network with beacon and network with primary exclusive regions.

Assuming that in a circular network the CRs are uniformly distributed with a constant density λ, the interference generated by these CRs depends on their locations and on the random channel fading, so this type of configuration causes random interference [31]. In the network with beacons where CRs capture and detect beacons sent from PRs, the CRs try to avoid transmitting in the next duration after successfully detecting these beacons. The PRs' communication is hence safe from

being perturbated. However, again the channel fading problem could make these CRs misdetect the beacons. Therefore, a beacon detection threshold becomes on a crucial parameter to design a CRN that limits the impact on the PR's operation. In the network with primary exclusive regions, the PR transmitter's exclusive region is better avoided by any CRs within the area since PR receivers within this area are passive devices and they might be affected if any of the nearby CR operates.

Also depending on the locations of CRs and PRs, our work studies the network environment's observations from the CRs point of view to evaluate the impact, which an on-going CRN may cause to the primary network. Our observations take into account the inclusive zone between PRs' and CRs' networks. This awareness is then incorporated into a metric called interference level that reflects the importance of the impact. Our proposed routing solution uses the interference level as the crucial metric on select the route that minimizes the impact to the primary networks that is unnecessarily completely avoided when inactive or non-existing PR receivers are detected. Our routing proposition is also a cross-layered approach where the network layer accesses and retrieves physical information directly from the physical layer via a management controller (see Section V-B). In the following sections, we detail the different parts of our work: overlap observation, impact estimation and routing proposal.

III. Overlap Region and Node Density Observations

In this section, we present the overlap region observation and node density estimation approach, which are the essential piece of information to envisage possible interference on the PR's system when CR's system is operating.

A. Overlap Region Observation

We argue that when the reception area of a CR emitter and the reception area of a PR emitter overlap, it produces unavoidable effects on the primary system, especially to the PR receivers. This observation was mentioned in [8]. However, we also proved that not only the overlap size but also the number of existing primary receivers cause the impact [9]. Our approach takes into account the overlap ratio and node density probability as two main factors. The ratio of the overlap size to the overall size of the PR emitter's disk is named overlap ratio, while the node density probability is the probability of possible node density within this PR emitter's disk.

The realistic overlap case highlighted in Figure 4 and Figure 5 is obtained when the following condition is satisfied. We study the possible impact of these general cases.

$$d < R_P + R_C \quad and \quad d > R_P \quad and \quad d > R_C. \tag{1}$$

The overlapping region is clearly displayed and by using classical geometry, we calculate the general overlap region between the PR and CR for this case in equation (2),

$$\begin{aligned} A_{Overlap} = & \frac{\theta_C}{2} R_C^2 - R_C^2 |\cos\beta| \cos\frac{\theta_C}{2} \\ & + \frac{\theta_P}{2} R_P^2 - R_C |\cos\beta| R_P \cos\frac{\theta_P}{2}; \end{aligned} \tag{2}$$

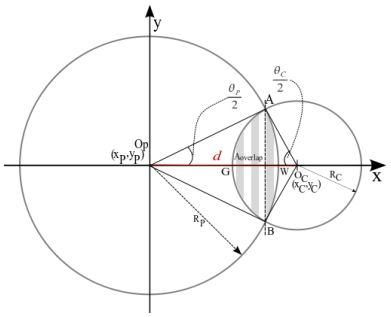

Figure 4. General overlap case

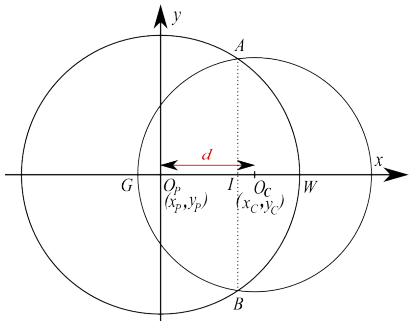

Figure 5. Particular overlapping case between PR Transmitter and a CR Node

where θ_C and θ_P are the angles formed at O_C and O_P with points A and B, respectively, whereas β is an intermediate variable for our computation given,

$$\begin{aligned} \sin\beta &= \frac{R_P^2 - \left(R_C^2 + x_C^2 + y_C^2\right)}{2 * R_C * \sqrt{x_C^2 + y_C^2}}; \\ \sin\frac{\theta_C}{2} &= \frac{R_C}{R_P} * |\cos\beta|; \\ \sin\frac{\theta_P}{2} &= |\cos\beta|. \end{aligned}$$

However, the case where $d < R_C < R_P$ shown in Figure 5 is not included in equation (2). This particular situation is captured in equation (3).

$$\begin{aligned} A_{Overlap} = & \frac{\theta_P}{2} R_P^2 - R_C R_P |\cos\beta| \cos\frac{\theta_P}{2} \\ & + \Pi R_C^2 - \frac{\theta_C}{2} R_C^2 \\ & + R_C^2 |\cos\beta| \cos\frac{\theta_P}{2}. \end{aligned} \tag{3}$$

Following up with the experiments, we present some associated results in this section. Figure 6 shows results for a scenario where over a single channel network we modify the overlap size and study its impact on PR receivers. PR receivers were uniformly deployed around the PR emitter. The x−axis illustrates the size of the overlap obtained from the location of the CR sender and calculated based on equations (2) or (3); the y−axis shows the ratio of impacted primary nodes. Lower coverage area in Figure 7 produces almost the same observed results on the single channel experiments.

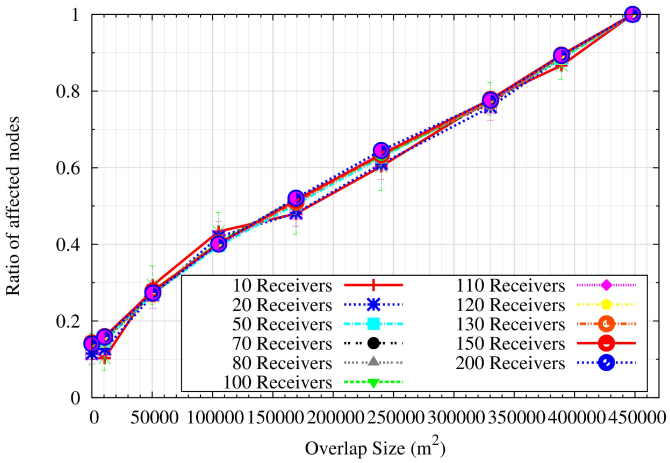

Figure 6. Single Channel - Different Overlap regions - Uniform Distribution

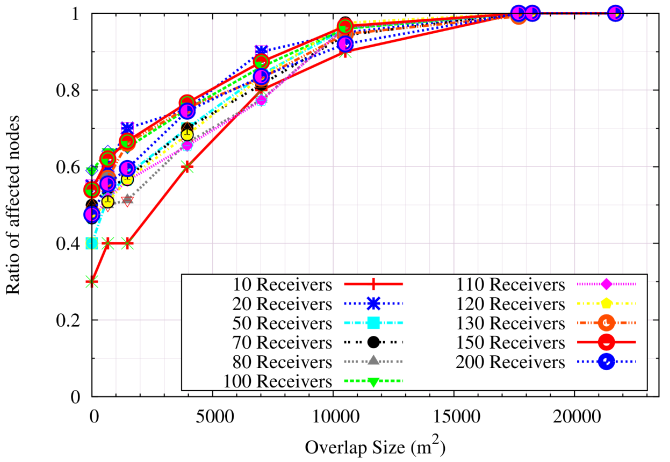

Figure 7. Single Channel - Different Overlap regions, smaller reception zone - Uniform Distribution

Figure 8 corresponds to the second scenario where two channels are available with a PR transmitter observing different overlaps on each channel. In fact, the overlap on channel_1 is about $120000m^2$ while on channel_2 the intersection between transmitter circles is around $500m^2$. In Figure 8, we study the distinctive ratio of affected nodes while modifying the number of PR receivers on both channels.

Again, the experiment is performed with various numbers of PR receivers within the PR transmitter's disks on both channels. The x-axis shows the number of PR receivers while the y-axis illustrates the ratio of nodes being affected by the CR transmitter's signal. This ratio varies from 10% to almost 15% on channel_2 but from almost 34% to almost 40% on channel_1 when the receivers are distributed uniformly within these disks (as in Figure 8).

Though the relationship between overlap sizes and the impact is shown, we performed another experiment on a single channel network with different overlap sizes and arbitrary

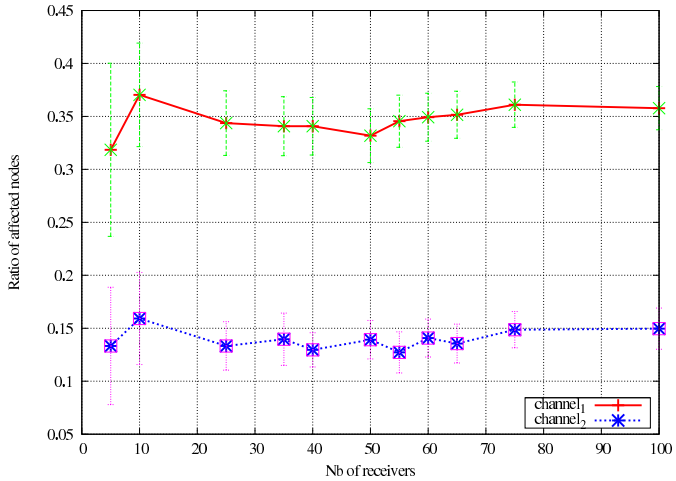

Figure 8. Multi Channel - Different Overlap regions - Uniform Distribution

deployment of PR receivers. In this test, the primary users were deployed further from the vulnerable area. For instance, even when 200 receivers were deployed, the ratio of affected nodes was lower than the deployment of 80 or 50 receivers in Figure 9 and Figure 10, respectively. Hence, envisaging the distribution over the overlap area and applying the proper prediction model to estimate the density of the receivers could be a new approach to protecting the primary receivers in general.

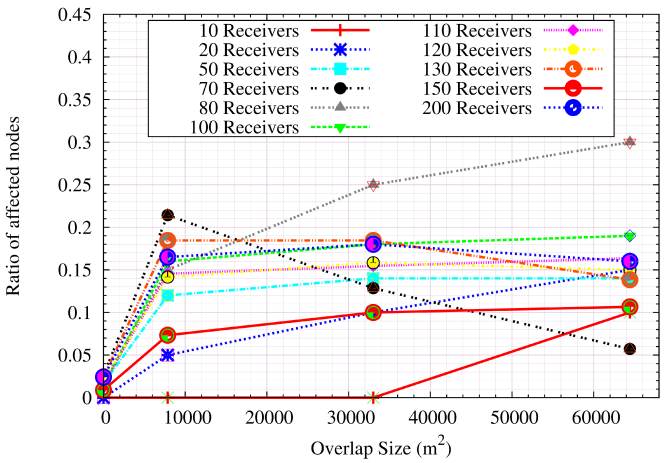

Figure 9. Single Channel - Big Reception Zone - Arbitrary Deployment

In summary, the simulation results reflect the relationship between the overlap area and the impact on the primary receptions with homogeneous distributions of PR receivers. However, positions of PRs may be affected by practical considerations such as obstacles, buildings, mountains, etc., which prevent regions of the coverage area from containing receivers. Therefore, a prediction model to estimate the location of these devices is required.

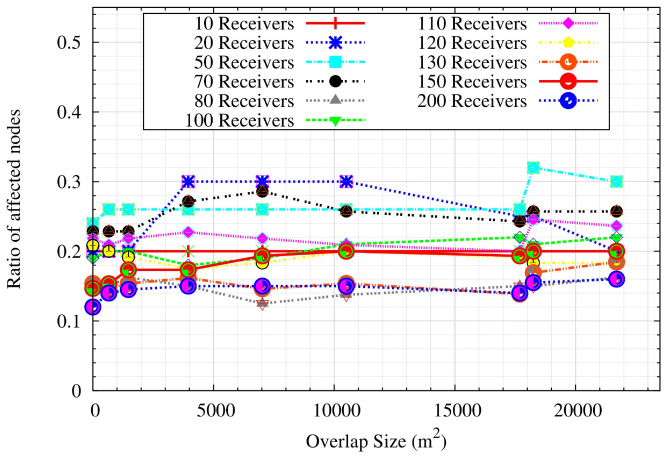

Figure 10. Single Channel - Small Reception Zone - Arbitrary Deployment

B. Node Density Estimation Approach

We now look for a solution for estimating the node density within a specific area. There are two approaches that are taken into account in this work the grey model GM(1, 1) and the Kalman filter. The Grey systems theory [32] is known for the analysis of problems with incomplete or uncertain information. This is an uncertain system in which the information is incomplete and the existing data is partially accurate. Grey system focuses on the uncertainty problems of known samples or inadequate information. Many components of Grey system theory have been built up since the theory was introduced in [33]. These components consist of systems analysis, evaluation, modeling, prediction, decision-making, etc. Our work focuses on the Grey prediction in terms of modeling and predicting on a set of samples.

In the literature, the Grey predictor is robust with respect to noise and lack of modeling information compared to other prediction methods [34]. The Grey model definition is quoted [32]: "Grey models predict the future value of a time series based only on a set of the most recent data depending on the window size of the predictor assuming that all the data used in the models are positive and the sampling frequency of the time series are fixed." One of the most efficient Grey models in real time applications is GM(1, 1). The model GM(1, 1), pronounced as "Grey Model First Order One Variable", is the time series forecasting model in which the model is renewed when new data become available to the prediction model [34].

In next generation networks, e.g., software-defined radio networks or so-called CRNs, the resource exploration process on these devices has very limited information about radio environment. A prediction model that satisfies partial knowledge can be useful. The density of these devices for example is one of the important characteristics that a CR needs to estimate to avoid the maximum perturbation on the primary system. A proposal on the use of the Grey Model in [35] defined a function that facilitates the detection of free-bands by the mobile cognitive radio equipment dedicated to the real-time patient's monitoring. This work basically proposed a predictive strategy, which is based on machine learning techniques combined with the Grey Model system for performing a spectral prediction. Although we characterize the relationship between the overlap area and the effect on the primary system, the primary receivers' density within this vulnerable area is vaguely known. We argue that the Grey Prediction Model is able to estimate the mobile node position.

Firstly, we are interested in predicting the distribution of the PR receivers within a specific area using the forecasting model GM(1, 1) and the Kalman filter. Since we are short of space in this article, we encourage readers to refer to details of the model GM(1, 1) explained in [9], and [35]. The model uses least-squares method to adapt the prediction curve to the original curve. The idea of using the least-squares method is to find the most closest point to the actual value curve/line of the data. In the Grey Model, to ensure the accuracy of the predicted value in the time domain (that reflects the trend of the series) and prediction control variation (the variance of the predicted value and the actual value), the least-squares method is applied to calculate these coefficient factors.

We adapt GM(1, 1) to predict primary receivers on a specific area if a statistical receiver quantity is known. Assuming we have statistical information of the number of active licensed mobile devices in a specific area (note that we focus on the rural area since there are less obstacles in-between). Depending on the time unit of the statistic, we extract the statistic into a time series chain of the number of active licensed devices, which is named "predicted PRs". This is the input series of the Grey Model GM(1, 1). In current experiments, the relationship between transmission power and reception power in free space can be approximated by [36]:

$$P_r(d) = \frac{P_t G_t G_r \lambda^2}{(4\pi d)^2 L}$$

where P_r and P_t are received and transmitted power, respectively, G_r and G_t denote the antenna gains of receiver and transmitter, L the system loss factors (a.k.a. filter losses and antenna losses), d the distance between the transmitter and the receiver and λ is the wavelength of the transmitted signal in meters. Thus, knowing the PR's positions based on their transmitting/received power by the CR node, the system (i.e., Cognitive Radio emitter) could estimate the changes in their position and the number of PR receivers from the overlap region. According to this information, the CR node could adapt its transmit parameters (power) to minimize the possible impact on PR systems.

Another approach that we consider is the Kalman filter. The Kalman-based estimator provides good results in practice due to its optimality (it minimizes the mean square error of the estimated parameters). The Kalman filter recursively corrects the estimation function associated with the current measured value, current predicted value and current predicted measurement value. For example, suppose we have a prediction function of variable x at time t called, $\hat{x}_t^-$. The current measured value is z_t, the predicted measurement, which is yielded by the predicted value of x at t is ${z^-}_t$, providing that ${z^-}_t = H{x^-}_t$ with H is the related matrix to the measured value at time t.

If the actual value of x is denoted by $\hat{x}_t$, the prediction function is then corrected as follows:

$$\hat{x}_t = \hat{x}_t^- + K(z_t - H\hat{x}_t^-) \quad (4)$$

K is called the Kalman gain associated with the error from the actual measured value and the prediction measurement value, z_t and $z^-{}_t$, respectively. In (4), the composition after K is the correction for the predicted function for estimation of x, denoted by $\hat{x}_t^-$.

We apply the same adaptation and series to perform an experiment with the basic Kalman filter model. The idea behind comparing these two methods is the data smoothing process that the Kalman filter provides. We found that the rendered plots provide similar effects between the original series and the predicted series. The collected results in Figure 11 and Figure 12 show the relationship between the received signal and the distance. The future position is predicted based on this received signal and the current position. These examples (Figure 11 and Figure 12) allow us to estimate the different positions of the PRs in the overlap region and to characterize the overlap region with PRs mobility. The sensitivity range for this case has a limit which approaches $-100dBm$. These results can also be the basis for adaptive transmission power selection.

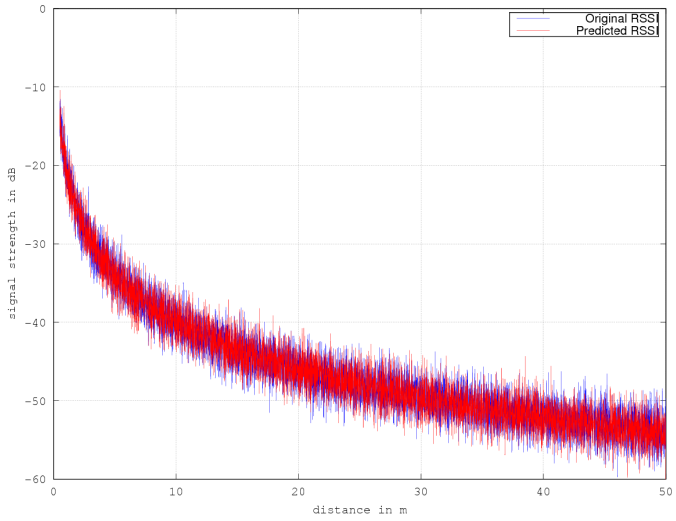

Figure 11. Relation of RSSI and distance with Grey Model GM(1, 1)

IV. Fuzzy Logic-based Interference Level Estimation

From the observations presented in the previous section, we combine overlap ratio and node density probability using fuzzy logic in this section. These parameters are the fuzzy inputs of our fuzzy inference system. A proper implication is applied for each rule listed in the rule table. The result from the implication rule is then aggregated and defuzzified to obtain the final result. This is the degree of impact on the primary system. A CR can consider this degree before using a frequency range when overlap happens.

To interpret the output of antecedents (i.e., the overlap ratio), we use the Mamdani Min Implication rules [7] to extract

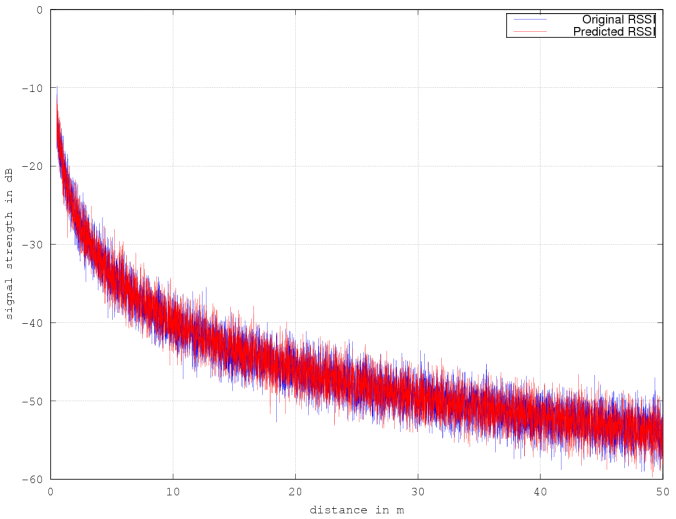

Figure 12. Relation of RSSI and distance with Kalman Filter

the final result for the overlap ratio fuzzy set. For instance, at the intersection of two functions, an *or* operator is used to connect two sets, and the maximum of two membership functions is evaluated for the antecedent part of the fuzzy rules.

$$\begin{aligned} \mu_{OverlapRatio}(x) &= \mu_{Low}(x) \vee \mu_{High}(x) \\ &= max[\mu_{Low}(x), \mu_{High}(x)] \end{aligned} \quad (5)$$

Detailed explanation and implementation to produce the interference level was described in our article [1], hence we only summarize the sample rules table, its inferred statements and the final results of the aggregation process to produce the interference level from the overlap ratio and node density probability.

TABLE I. ENHANCE INTERFERENCE LEVEL RULES TABLE

Index	Overlap Ratio	Density	Interference Level
1	Low	Low	Low
2	Low	Medium	rather Medium
3	High	Medium	somewhat High
4	High	High	High
5	Very High	High	extremely High
6	Very High	Very High	extremely very High

For instance, the above rules infer the following.

- If (Overlap-Ratio is *Low*) or (Density-Ratio is *Low*), then (Interference Level is *Low*) (1)
- If (Overlap-Ratio is *Low*) and (Density-Ratio is *Medium*), then (Interference Level isn't *Low* or rather *medium*) (0.5000)
- If (Overlap-Ratio is *High*) or (Density-Ratio is *Medium*), then (Interference Level is somewhat *High*) (1)
- If (Overlap-Ratio is *High*) or (Density-Ratio is *High*), then (Interference Level is *High*) (1)

- If (Overlap-Ratio is Very *High*) and (Density-Ratio is *High*), then (Interference Level is extremely *High*) (1)
- If (Overlap-Ratio is Very *High*) or (Density-Ratio is Very *High*), then (Interference Level is extremely Very *High*) (1)

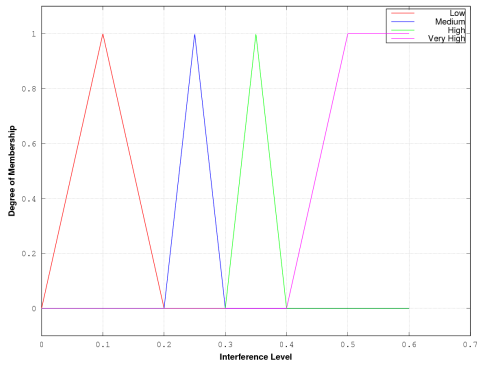

Figure 13. Interference Level membership function

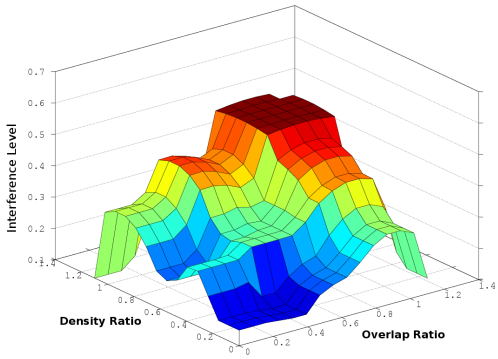

Figure 14. Interference Level Output as function of Overlap and Node Density - Rule set of 16

The fuzzy inference engine combines the rules to obtain the aggregated fuzzy output. The output is the fuzzy set of the interference level that is defined in Figure 13. The Fuzzy controller has to defuzzify this output into crisp values using the centroid method to make the final decisions. Figure 14 shows the system output as a function of 2 variables, overlap ratio and node density, with the rules set of 16 conditional statements.

Table II and Table III show the fuzzified data of the inputs based on their defined membership functions. Table IV shows the output of the inference system. The aggregated values are processed according to the interference membership function in Figure 13. The rules are applied correspondingly in the defuzzification process to produce the final crisp value of the interference level.

More precisely, the Fuzzy Logic Controller (FLC) maps the fuzzified outputs (a.k.a., the output of each linguistic variable of overlap ratio and node density probability) of the inputs to infer the associated consequences. For instance, the inference engine decomposes an input of overlap ratio of 0.25596 into

TABLE II. OVERLAP DEGREE FUZZIFICATION OUTPUT

Index	overlap ratio	$\mu(x)$ Low	$\mu(x)$ Medium	$\mu(x)$High	$\mu(x)$ Very High
1	0.25596	0.29362	0.37305	0	0
2	0.57829	0	0	0.81143	0
3	0.44402	0	0.37322	0.29345	0
4	0.66566	0	0	0.22894	0.26264
5	0.53420	0	0	0.89467	0
6	0.65453	0	0	0.30314	0.21811

TABLE III. DENSITY DEGREE FUZZIFICATION OUTPUT

Index	Density probability	$\mu(x)$ Low	$\mu(x)$ Medium	$\mu(x)$ High	$\mu(x)$ Very High
1	0.08049	1	0	0	0
2	0.19908	0.67281	0	0	0
3	0.66764	0	0	0.21574	0.27056
4	0.81842	0	0	0	0.87370
5	0.28182	0.12118	0.54548	0	0
6	0.57480	0	0	0.83466	0

TABLE IV. INTERFERENCE LEVEL FUZZIFICATION DATA

Index	Overlap input	Density input	Interference Level	Crisp Value
1	0.25596	0.08049	Low	0.14236
2	0.57829	0.19908	Medium	0.21464
3	0.44402	0.66764	High	0.39495
4	0.66566	0.81842	Very High	0.47103
5	0.53163	0.74970	Very High	0.40053
6	0.65453	0.57480	High	0.37930

$\mu(low)$ at 0.29362 and input of density probability of 0.08049 into $\mu(low)$ at 1. This composition matches the first rule in Table I - *If (Overlap-Ratio is Low) or (Density-Ratio is Low), then (Interference Level is Low).*

Figure 14 shows the system output as a function of 2 variables, overlap ratio and node density, and the output of interference level. Each of the variables presented in Figure 14 reflects both the linguistic and also the crisp values. For instance, when the overlap degree and density degree are zeros, the interference is also almost zero (coded with dark-blue area). While the overlap ratio is high (over 60% certainty) and the node density degree is low (below 20%), the interference level is low with low probability (the blue area). This explains the fact that the interference level still strongly connects to the 20% degree of node density that might be affected by the big overlap ratio. The higher the node density, the higher the interference level with high probability.

This interference level can be used in routing in CRNs, which we present in the next section.

V. ROUTING DESIGN PROPOSITION

To get the picture of current work for routing in mobile networks, we go through some existing approaches for routing solutions. There exist three types of routing protocol designs for mobile networks: proactive, reactive and hybrid. Proactive routing protocol are protocols that require node establishes a route to all destinations regardless of the applications' demand. In reactive routing protocol, on the other way round, a node only initiates routing explorations upon applications' demand. Hybrid protocols merge the advantages of both proactive and reactive features.

On Link State Routing (OLSR) is a well-known proactive routing protocol while Ad-hoc On-demand Distance Vector (AODV) and Dynamic Source Routing (DSR) are common

reactive routing protocols. However, which routing protocol can work efficiently in CRNs and how much adaptation could be considered? There are some considered facts in cognitive radio ad-hoc network routing design, as follows. Routing protocol in CRNs should

- avoid periodic messages since redundant messages sometimes cause collision and confusion,
- avoid acknowledgement over the CR link, so that the overhead of the protocol is not too big,
- detect primary users' existence so that the routing exploration process does not cause serious impact to the primary networks.

We first look at some current research that studies the performance of reactive routing protocols. In literature, much work has been conducted to verify the efficiency of these reactive protocols but obtained results are controversial. We present some of the work in the following.

Johnson and David [37] introduced DSR in 1996 and the protocol was then standardized in RFC 4728 [38] in 2007. DSR was designed to quickly adapt to routing changes when a mobile host moves frequently in an ad-hoc network. A route establishment process can only initiate on the desire of the data sender - when a host wants to send a data packet to a destination.

AODV was introduced in 1999 by C. E. Perkins, E. Belding-Royer, and E. M. Royer [39] and was standardized in RFC 3561 [40]. The original design of the protocol has been vastly used by the research community. Many spin-off of AODV have been proposed as the routing protocol for different types of mobile networks.

In principle, AODV is a table-driven routing protocol while DSR is cache-driven. AODV has route maintenance features while DSR lacks route maintaining function. DSR has to re-initiate the routing exploration process when there is a link breakage. Consequently, data communication may be interrupted.

AODV's creator and his co-authors conducted a comparison regarding the performance of these two routing protocols in ad-hoc modes in [41]. Packet delivery fraction (or ratio in some of the recent articles), average end-to-end delay and normalized routing load were the main metrics used to measure the performance of AODV and DSR. The performance results show that DSR outperforms AODV in small network topology and lower mobility. However, AODV handles changes better - i.e., nodes move faster - than DSR does in dynamic networks thanks to the tracking mechanism. Basically, since AODV keeps track of actively used routes, multiple actively used destinations can hence be searched using a single route discovery flood. This mechanism helps to control routing load over the medium, so that the overhead of the protocol seems to be lower than that of DSR. However, the overhead may come from MAC instead causing the routing load increases.

Recently, Jain et al. redo the comparison of these two protocols on the basis of propagation path loss models [42] while Manickam et al. in [43] examine the performance of these two protocols similarly to the work of Perkins et al. in [41].

TABLE V. ROUTING PROTOCOL COMPARISON TABLE

Protocol	Type	Metric	Periodic message	Acknowledgement message	Applicable network
DSR	Reactive	Shortest path	Yes	Yes	Ad-hoc but less dynamic than AODV
OLSR	Proactive	Shortest path	Yes	Yes	MANETs
AODV	Reactive	Hop count	Yes	Yes	MANETs
DYMO	Hybrid	Hop count with alternative metrics	No	Optional	VANETs and MANETs

The concluded results suggest similar performance to that described in [41]. Yet in [42], [43], DSR has lower end-to-end delay than AODV since the exploring path from source to sink is attached in every routing request. By reversing the enclosed path, the sink does not take much time to travel back to the source, so that the processing delay is reduced. Regarding the packet delivery fraction, AODV performs consistently better than DSR does in both [41], [43].

Regarding the performance of a proactive and a reactive routing protocol, we found a study of Sagar et al. [44] in which OLSR is compared with Dynamic MANET On-demand (DYMO) or AODVv2 routing protocol. DYMO was designed to deal with modern day dynamic ad-hoc network topologies. It works as a reactive and also a proactive routing protocol. Initiating discovering routes when it is active or looking up for a route on demand are two different configurations of DYMO. In fact, the protocol is intended for use by mobile routers in wireless, multihop networks. DYMO operates very similarly to AODV, but requires only the most basic route discovery and maintenance procedures [45]. DYMO has also been built with enhancements. Most of the optimizations available in AODV should be applicable to DYMO as well. Sagar et al. [44] have evaluated DYMO and OLSR on MANETs and VANETs. The results suggest that DYMO performs better than OLSR does especially in VANETs where the mobility of mobile nodes are dynamic and the surrounding is quickly changed. Other analyse on the performance of DYMO are also discussed in [46], [47]. All these works concluded that DYMO outperformed the existing routing protocols for MANET in terms of packet delivery, delay and compatible throughput. However, in [45] the authors suggest that DYMO assumes the link between mobile nodes are bidirectional. More precisely, this routing relies on the accuracy of the information provided from the MAC layer.

Overall, a proactive routing protocol requires that a route is established and maintained before any data communication is needed. Therefore, it may not be suitable for CRNs due to the overhead of the control messages all over the channels. Consequently, the resources of a cognitive node exploits may just be used for routing the control message. However, with a reactive routing protocol, the route exploration process is only initiated when a node wants to start a data communication, though route maintenance should be also considered as part of the design. We want to leverage current design with minimal customization. Therefore, adopting both reactive and proactive approaches appears to be reasonable. The DYMO protocol is a potential candidate for this purpose. We will briefly discuss the protocol and its essential operations; e.g., route discovery and route maintenance.

A. DYMO Operation

The Dynamic MANET On-demand DYMO routing protocol has been developed and defined as an IETF specification

(Internet draft version 4.0) [48]. This is a successor of the AODV routing protocol, which was proposed by the same main author. DYMO has AODV's attributions, which can work basically in mobile ad-hoc network mode. For instance, route discovery is only activated when needed. Loop prevention is done by attaching the sequence number to each routing message. Supposedly, a node only creates a route when it has a demand to send data messages to the target node. Therefore, the intermediate nodes maintain and detect topology changes while listening to these exchanging data messages. No HELLO packets are needed to distinguish AODV, so the change is detected faster and the overhead of sending extra control messages is lower. However, some requirements of DYMO should be taken into account to guarantee the best performance of this protocol. The protocol assumes to work under the bidirectional link. It hence relies on the reliability of the lower layer to provide essential environment state information. We will discuss this relation in later Sections. Firstly, we briefly describe the main operations of DYMO in MANET.

Route Discovery: When a mobile node wants to establish a path to communicate to another node in the network, this node has to discover the path to reach its desired destination. To do so, this node, called the source, generates a route request and transmits this request to any of its known neighbors. Each of these neighbors, including the source and the target node, will maintain the active discovered link via a routing table, which is created right after the discovery process finishes. Each entry contains basic information for routing such as the addresses of source and sink, sequence number, hop-count, next hop address, next interface, timestamp of last used, expiration time, metric type and metric, the route state.

We provide an example in Figure 15 to comprehensively illustrate the route discovery process of DYMO in MANET. A path must be established to allow routing data from A to F. Similar to AODV, routing information is maintained at A in its own routing table while RREQ is flooded to A's neighbors and their other neighbors until the destination is reached. The sequence number in each RREQ is increased at each new neighbor before the RREQ is forwarded. At C, there are redundant RREQs from both directions with the same sequence number. If the alternative metric was not pre-set, it does not matter which path will be chosen. In this case, let us assume that C records the route from B to C. C then carries on forwarding this RREQ to the next hops, D and F. F is already the target destination while D is not. F replies the request with its RREP while D records the route. The RREP from F will be transferred on the reverse path from F back to C, B and A, the source. The data transmission will be then followed after this process has finished.

Upon sending the RREQ, the originator node A has to wait for a RREQ WAIT TIME for the RREP reception. In case there is no RREP received, A properly attempts to send another RREQ with a different sequence number. The waiting time is set to be 1000 milliseconds by default. Once the RREP is created and sent back, the flow of traffic of RREP is unicast. Therefore, it relies heavily on the MAC to ensure the bidirectional link underneath the network layer.

An example scenario of a CRN without PR is depicted in Figure 15. Since DYMO allows us to implement an alternative metric for the route selection process, we can modify the

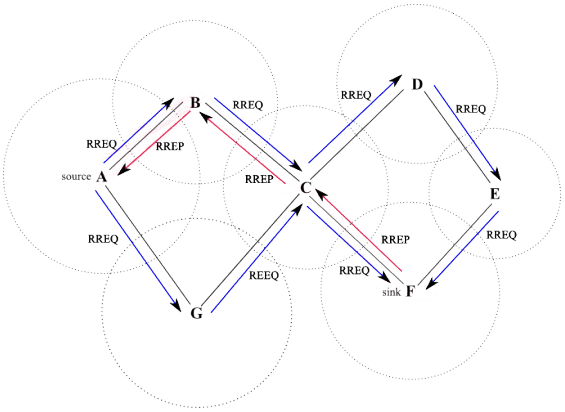

Figure 15. DYMO Route Discovery from source A to sink F without PR's existence

protocol with a minor change in retrieving MAC information according to the environment observations explained previously. An example of the application that DYMO can work in CRN is illustrated in Figure 16, in which we assume that B is kept in silent as it operates in the area where it overlaps with a PR transmitter. This is an expected route discovery with a scenario of a CRN with PR's existence depicted in Figure 16 using an alternative routing metric interference level.

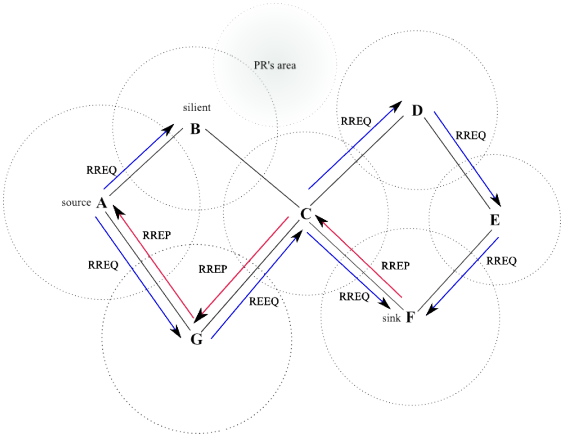

Figure 16. DYMO Route Discovery from source A to sink F with PR's existence

Route Maintenance: Each node that has received a route request and a route reply has to maintain the active route locally by monitoring the communication exchanging along the path. However, when there is problem in the network that triggers the path changes, a route error (RRER) may be generated and issued by these nodes to their neighbors. Two common problems are broken links on the current active route and unknown path from a received data packet.

Before using a route to forward a packet, a node must check the status of the route as follows. If the route is marked as broken, this node will not use it for forwarding. If the $Current\_Time$ is higher than the $Route.ExpirationTime$, the route has expired and cannot be used for forwarding. If the route is currently not in use when $(Current\_Time - Route.LastUsed) < (MAX\_SEQNUM\_LIFETIME)$,

the route table entry must be expunged. When generating a RRER, a node creates a list of unreachable destinations including their addresses with associated sequence number. Its routing table is also updated according to the broken link.

In the case of undeliverable packets, the RRER may be multicasting or unicasting to the neighbor from which the data packet was sent from. For unicast RRER, a special message type of value (TLV) is mandatorily included. In the case of broken link, the RRER is sent to all neighbors of the node that experience a broken link. After the other intermediate nodes receive the RRER, they verify the information contained in the RRER to react with the event accordingly. We illustrate this process in the example in Figure 17. A Route Error RRER is generated from C and then sent towards all of C's neighbors including B, G, and D to prevent future data transmission towards link C-F. These nodes had already recorded a path containing F; therefore, the RRER is further sent to A and E.

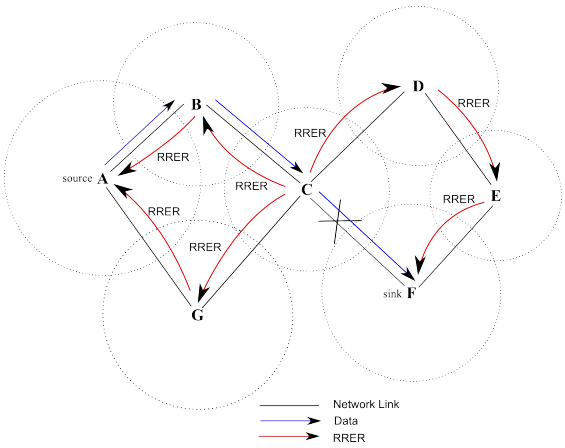

Figure 17. DYMO Route error sent from C when there is a broken link

The Hop Count is traditionally used as the default metric to select a route for a target node in exisiting table entries. However, some applications may require metric information other than Hop Count and this metric unfortunately sometimes causes the selection of the worst possible route in many situations. In CRNs, sometimes the Hop Count metric is not sufficient to choose a route to a target without interfering with current operating primary networks. The authors of AODVv2 [48] have been discussing alternative metrics since 2012. It was introduced in Internet draft version 24 [49]. Each such alternate metric measures a "cost" of using the associated route, and there are many different kinds of cost (latency, delay, monetary, energy, etc.).

The cost of each of the multiple routes is measured by a different metric. The specification provides the abstract function to evaluate the cost of each route in term of a function $Cost(R)$, where R is the route for which the cost is calculated. The route information for R must always include the type of metric by which $Cost(R)$ is evaluated. While using this alternative metric, we should also be careful and guarantee a loop-free environment while the routing engine is operating. In other words, given that the $Cost(R)$ is calculated, a loop-free routine should also be invoked. Since DYMO-AODVv2 is still work in progress, specific descriptions for metric type for alternative metric vaguely describes. The protocol requires experiments and changes if necessary. In the scope of this work, we tend to use it to evaluate the efficiency of interference level in preventing impact on PR networks while the routing engine is working.

B. CRN-DYMO routing protocol

Generally, our working scope is a conceptual framework that is illustrated in Figure 18. This framework focuses on an interference avoidance strategy which co-exists between the CRN and primary network scenarios, providing that the *Management Controller* stores all environments' observation parameters such as mobile nodes' movements and locations. The *Overlap Calculation* block then can locally retrieve, compute and analyse the current situation of the current CR compared to a PR emitter. Similarly, the *Node Density Estimator* obtains historical statistics of the node within a specific area and estimates the probability of current node density. These blocks produce estimated inputs for the *Interference Estimator*, which combines these inputs using fuzzy logic to compute the interference level.

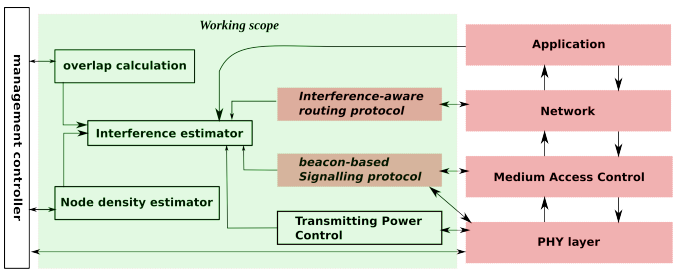

Figure 18. Working scope

Essentially, the DYMO routing agent can retrieve its neighbor's information based on the MAC layer and the interference level from the *Interference Level Estimator*. Customized DYMO-CRN the attaches interference level as an alternative metrics that is used for route selection, as explained in Figure 19 and Figure 20.

In Figure 19, we describe the route discovery, which is performed at node A to look for a path to node E overlapping with a PR. We assume that at C, the sequence numbers in the RREQs are the same for both direction from B to C and from G to C, but the interference levels from B and D are medium with non-zero probability. Therefore, in this case, the selected path to E is the path towards F. Figure 20 has the similar scenario with Figure 19 with an overlap with PR2 on G's and F's side. Route selection is changed since the interference levels from B and D are medium with non-zero probability while the interference levels from G and F are high with non-zero probability, and the interference level from C with PR2 is small with non-zero probability.

C. The routing process of Dymo-CRN routing protocol

We propose an extended Dymo routing protocol for CRN in this section. The proposed protocol involves route discovery and route maintenance processes.

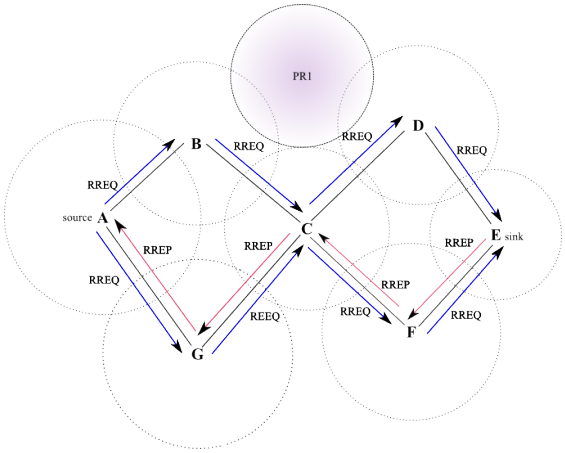

Figure 19. DYMO Route Discovery from source A to sink E with PR's existence

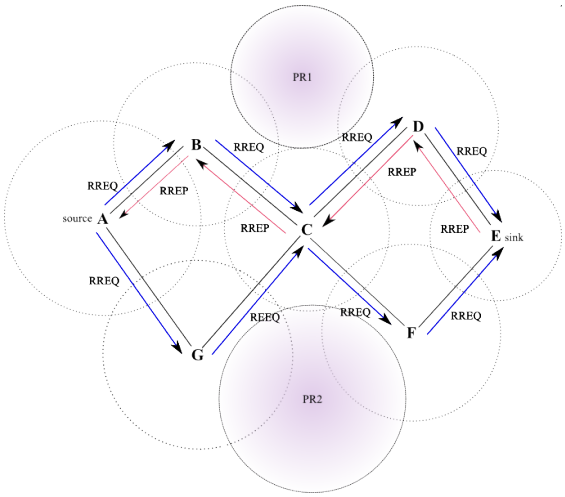

Figure 20. DYMO Route Discovery from source A to sink E with 2 PRs' existence

1) Route discovery: Similarly to Dymo specification, route discovery of the proposed protocol is performed when a node must transmit a packet towards a destination for which it does not have any route. The discovery process initiates and multicasts a route request message (RREQ) to find a path toward some target destination. Along the path, each of the neighbor who receives the request records a route toward the originator. When the request reaches the target node, this node also records the path included in the request and generates a unicast route reply (RREP) to the originator. Again, each neighbor along the path receiving this reply also records the path toward the target destination of the previous RREQ. These intermediate nodes then send the RREP unicast to the originator. The citeria to evaluate incoming route information are the hop count and the interference level (IL), which is the alternative metric. When a RREQ is received, each node will check, acquire its local interference level on each channel assuming that the node may have more than one available accessible channel. A comparison among its local IL is carried out and the most optimal IL is chosen as the local $metric\_IL$. As well as hop_count, the new_metric and new_metric_IL are recalculated as in (6) and (7). As presented, IL is a impact level computed from the percentage of overlap and node density degree. The new metric hence takes the average IL of the current local IL and the received IL. This is the metric of IL for the path from the orignator to the current node.

$$new\_metric\_IL = (metric\_IL + last\_metric\_IL)/2 \quad (6)$$

$$new\_metric = metric + last\_hop\_metric \quad (7)$$

The information from a received RREQ is handled by a routine call routing handling process (RteHandler), as described in Figure 21. By default, DYMO uses hop count as the routing metric to handle a route request with metric type 3. In the context of this work, we define metric type 4 to be the metric type of interference level. A metric type message TLV should hence be built and attached to a route message accordingly. During the RREQ process, the handler checks and looks in its routing table for an entry with the extracted metric type, e.g., metric type 4 for IL. In addition, an optimal IL is also acquired locally at the current node to recompute the new metric cost along the path. If the path to the target node exists, the sequence number of the entry is then compared with the sequence number in the received RREQ. In the end, the process will return an existing route entry without any update if the sequence number of the RREQ is outdated or the metric in the RREQ does not improve the cost of the path. If the routing entry needs to be updated (e.g., the sequence number needs to be refreshed, status of the route and update the new metric value). The routing table is also updated accordingly. The merit of enabling the metric IL is that we can guarantee the optimal IL from each CR to the its surrounding. If the current path has the minimum IL along the path, the route from the original CR to the target CR should have the least impact on any PR receivers.

2) Route maintenance: Route maintenance is performed to avoid permaturely expunging a route from the current route table as well as to avoid dropping packets when an active route breaks. Basically, the maintenance process consists of two operations, extending the route lifetimes upon successfully forwarding a packet and notifying the upstream nodes when a route to a target is broken due to loss of link to neighbors. In CRNs, breaking link to neighbors could be due to environmental change such as the transmission of PR receivers. However, thanks to the information obtained from the radio event table, CR nodes can always look for an alternative route and start notifying their neighbors about the change. This change would result in a complete path change (via different channels). The discovery process may be invoked in the case of one of the nodes is unreachable. This work can be deferred to future work.

VI. Conclusion

Overall, we have presented the entirely of a routing strategy in CRNs. The article covers everything from the simplest observation of the surroundings regarding the overlap phenomena and primary node density with associated techniques. These observations are inputs to produce a routing metric that could prevent foreseen interference when a CRN coexists

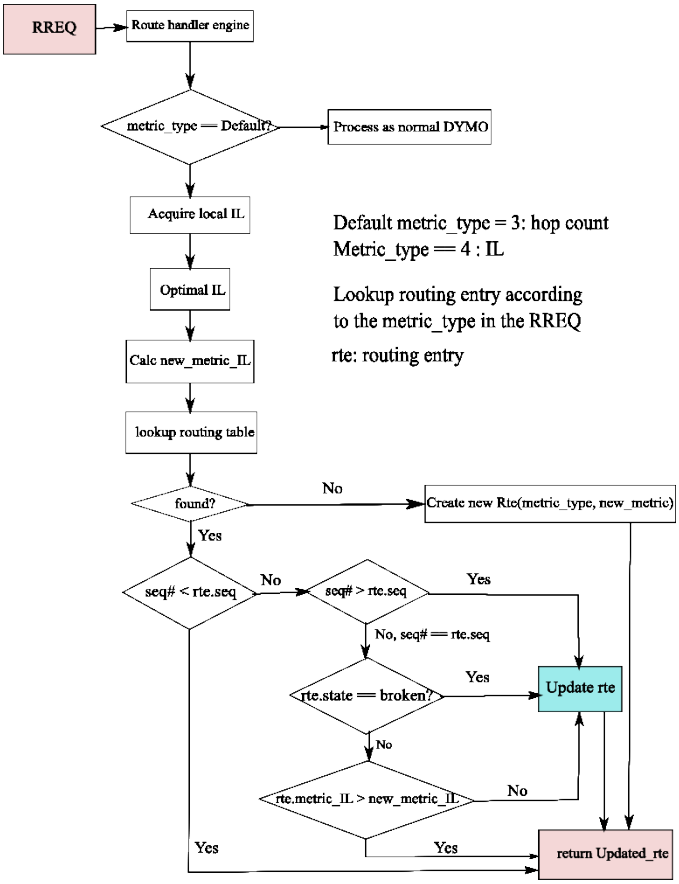

Figure 21. Routing information process

with a primary network. Essentially, we introduced a medium access control messages dissemination procedure, in which CR nodes maintain the knowledge of their neighbors as well as their resources before they can initiate transmissions. This establishment supports the routing protocol at the upper layer, which in this case is the interference level routing protocol. This is a guideline for developing a cognitive routing protocol that could prevent potential impact on primary networks when CRNs operate. Further extension of this work is encouraged to provide a more elaborate protocol so that it can be applied in a real CRN platform.

ACKNOWLEDGMENT

This work is supported by LICoRNe project, funded in part by the National Agency for Research in France - ANR (Agence Nationale de la Recherche). Besides, the authors would like to thank Dr. Yao-ban Chan of University of Queensland for proofreading.

REFERENCES

[1] M. T. Quach, F. Krief, M. A. Chalouf, and H. Khalifé, "Fuzzy-based interference level estimation in cognitive radio networks," in The Tenth Advanced International Conference on Telecommunications (AICT). IARIA XPS, 2014, pp. 138–143.

[2] M. J. Copps, "Bringing broadband to rural america: Report on a rural broadband strategy," Federal Communications Comission, Tech. Rep., May 2009.

[3] F. C. Comission, "Bringing broadband to rural america: Update to report on a rural broadband strategy," Federal Communications Commission, Tech. Rep., 2011.

[4] J. Genachowski, M. Clyburn, and J. Rosenworcel, "Eight broadband progress report," Federal Communications Commission, Tech. Rep. FCC 12-90, August 2012.

[5] I. F. Akyildiz, W.-Y. Lee, M. C. Vuran, and S. Mohanty, "Next generation/dymanic spectrum access/cognitive radio wireless newtork: A survey," in Computer Networks, vol. 50, 2006, pp. 2127–2159.

[6] D. N. Ekram Hossain and Z. Han, Dynamic spectrum access and management in cognitive radio networks. Cambridge University Press Cambridge, 2009.

[7] T. J. Ross, Fuzzy logic with engineering applications. John Wiley & Sons, Ltd., 2010.

[8] M. T. Quach and H. Khalife, "The impact of overlap regions in cognitive radio networks," in Wireless Days (WD), IFIP, 2012, pp. 1–3.

[9] M. T. Quach, D. Ouattara, F. Krief, H. Khalifé, and M. A. Chalouf, "Overlap regions and grey model-based approach for interference avoidance in cognitive radio networks," in IEEE Fifth International Conference on Ubiquitous and Future Networks (ICUFN), 2013, pp. 642–647.

[10] M. Cesana, F. Cuomo, and E. Ekici, "Routing in cognitive radio networks: Challenges and solutions," Ad Hoc Networks, vol. 9, no. 3, 2011, pp. 228–248.

[11] B. Wang and K. J. R. Liu, "Advances in cognitive radio networks: A survey," IEEE Journal of Selected Topics in Signal Processing, vol. 5, no. 1, Feb 2011, pp. 5–23.

[12] Q. Wang and H. Zeng, "Route and spectrum selection in dynamic spectrum networks," in IEEE Consumer Communications and Networking Conference (CNCC), 2006, pp. 342–346.

[13] H. Khalifé, N. Malouch, and S. Fdida, "Multihop cognitive radio networks: To route or not to route," IEEE NET, The Magazine of Global Internetworking, vol. 23, no. 4, August 2009, pp. 20–25.

[14] G. Cheng, W. Liu, Y. Li, and W. Cheng, "Spectrum aware on-demand routing in cognitive radio networks," in 2nd International Symposium on New Frontiers in Dynamic Spectrum Access Networks. IEEE, 2007, pp. 571–574.

[15] Y. Liu, L. Cai, and X. Shen, "Spectrum-aware opportunistic routing in multi-hop cognitive radio networks," IEEE Journal on Selected Areas in Communications, vol. 30, no. 10, November 2012, pp. 1958–1968.

[16] G.-M. Zhu, I. F. Akyildiz, and G.-S. Kuo, "Stod-rp: A spectrum-tree based on-demand routing protocol for multi-hop cognitive radio networks," in IEEE Global Telecommunications Conference, Nov 2008, pp. 1–5.

[17] A. Cacciapuoti, C. Calcagno, M. Caleffi, and L. Paura, "CAODV: Routing in mobile ad-hoc cognitive radio networks," in Wireless Days (WD), October 2010, pp. 1–5.

[18] S. Salim and S. Moh, "On-demand routing protocols for cognitive radio ad hoc networks," EURASIP Journal on Wireless Communications and Networking, vol. 2013, no. 1, 2013, pp. 1–10.

[19] C. Xin, B. Xie, and C.-C. Shen, "A novel layered graph model for topology formation and routing in dynamic spectrum access networks," in First IEEE International Symposium on New Frontiers in Dynamic Spectrum Access Networks. IEEE, 2005, pp. 308–317.

[20] S. Krishnamurthy, M. Thoppian, S. Venkatesan, and R. Prakash, "Control channel based mac-layer configuration, routing and situation awareness for cognitive radio networks," in Military Communications Conference (MILCOM). IEEE, 2005, pp. 455–460.

[21] Q. Guan, F. Yu, S. Jiang, and G. Wei, "Prediction-based topology control and routing in cognitive radio mobile ad hoc networks," IEEE Transactions on Vehicular Technology, vol. 59, no. 9, Nov 2010, pp. 4443–4452.

[22] K. Chowdhury and M. Felice, "Search: A routing protocol for mobile cognitive radio ad-hoc networks," Computer Communications, vol. 32, no. 18, 2009, pp. 1983–1997.

[23] K. Habak, M. Abdelatif, H. Hagrass, K. Rizc, and M. Youssef, "A location-aided routing protocol for cognitive radio networks," in International Conference on Computing, Networking and Communications (ICNC), Jan 2013, pp. 729–733.

[24] K. Chowdhury and I. F. Akyildiz, "Crp: A routing protocol for cognitive radio ad hoc networks," Selected Areas in Communications, IEEE Journal on, vol. 29, no. 4, 2011, pp. 794–804.

[25] E. Hossain, L. Le, N. Devroye, and M. Vu, "Cognitive radio: From theory to practical network engineering," in New Directions in Wireless Communications Research, V. Tarokh, Ed. Springer, 2009, pp. 251–289.

[26] T. C. Clancy, "Achievable capacity under the interference temperature model," in 26th IEEE International Conference on Computer Communications (INFOCOM), May 2007, pp. 794–802.

[27] M. Gastpar, "On capacity under receive and spatial spectrum-sharing constraints," IEEE Transactions on Information Theory, vol. 53, no. 2, Feb 2007, pp. 471–487.

[28] P. J. Kolodzy, "Interference temperature: a metric for dynamic spectrum utilization," International Journal of Network Management, vol. 16, no. 2, 2006, pp. 103–113.

[29] W. Wang, T. Peng, and W. Wang, "Optimal power control under interference temperature constraints in cognitive radio network," in IEEE Wireless Communications and Networking Conference, WCNC. IEEE, 2007, pp. 116–120.

[30] Y. Xing, C. Mathur, M. Haleem, R. Chandramouli, and K. Subbalakshmi, "Dynamic spectrum access with qos and interference temperature constraints," IEEE Transactions on Mobile Computing, vol. 6, no. 4, April 2007, pp. 423–433.

[31] M. Vu, S. Ghassemzadeh, and V. Tarokh, "Interference in a cognitive network with beacon," in IEEE Wireless Communications and Networking Conference (WCNC), March 2008, pp. 876–881.

[32] D. Julog, "The basis of grey theory," Huazhong University of Science and Technology Press, 2002.

[33] L. Sifeng, F. J., and Y. Yingjie, "A brief introduction to grey systems theory," in Grey Systems and Intelligent Services (GSIS), 2011 IEEE International Conference on, 2011, pp. 1–9.

[34] E. Kayacan, B. Ulutas, and O. Kaynak, "Grey system theory-based models in time series prediction," Expert Systems with Applications, vol. 37, no. 2, 2010, pp. 1784–1789.

[35] D. Ouattara, F. Krief, M. A. Chalouf, and O. Ahmdi, "Spectrum sensing improvement in cognitive radio networks for real-time patients monitoring," in International Conference on Wireless Mobile Communication and Healthcare (MobiHealth), November 2012, pp. 179–188.

[36] E. Hossain, D. Niyato, and Z. Han, "Dynamic spectrum access and management, cognitive radio networks," Cambridge University Press, 2009.

[37] D. B. Johnson and D. A. Maltz, Dynamic source routing in ad hoc wireless networks. Springer, 1996, ch. 5, pp. 153–181.

[38] D. Johnson, Y. Hu, and D. Maltz, "The Dynamic Source Routing Protocol (DSR) for Mobile Ad Hoc Networks for IPv4," RFC 4728 (Experimental), Internet Engineering Task Force, Feb. 2007, URL: http://www.ietf.org/rfc/rfc4728.txt [accessed: 2013-11-02].

[39] C. E. Perkins, E. Belding-Royer, and E. M. Royer, "Ad-hoc on-demand distance vector routing," in Second IEEE Workshop on Mobile Computing Systems and Applications. IEEE, 1999, pp. 90–100.

[40] C. E. Perkins, E. Belding-Royer, and S. R. Das, "Ad hoc On-Demand Distance Vector (AODV) Routing," RFC 3561 (Experimental), Internet Engineering Task Force, 2003, URL: http://www.ietf.org/rfc/rfc3561.txt [accessed: 2013-11-02].

[41] C. E. Perkins, E. M. Royer, S. R. Das, and M. K. Marina, "Performance comparison of two on-demand routing protocols for ad hoc networks," Personal Communications, IEEE, vol. 8, no. 1, 2001, pp. 16–28.

[42] M. Jain, J. I. Choi, T. Kim, DineshBharadia, S. Seth, K. Srinivasan, P. Levis, S. Katti, and P. Sinha, "Practical, real-time, full duplex wireless," in Proceedings of the 17th annual international conference on Mobile computing and networking. ACM, 2011, pp. 301–312.

[43] P. Manickam, T. G. Baskar, M. Girija, and D. Manimegalai, "Performance comparisons of routing protocols in mobile ad hoc networks," International Journal of Wireless & Mobile Networks, vol. 3, no. 1, 2011, pp. 98–106.

[44] S. Sagar, J. Saqib, A. Bibi, and N. Javaid, "Evaluating and comparing the performance of dymo and olsr in manets and in vanets," in IEEE 14th International Multitopic Conference (INMIC), 2011, pp. 362–366.

[45] C. Perkins and I. C. Futurewei, "Dynamic manet on-demand (AODVv2) routing," Internet-Draft, 2013, URL: https://tools.ietf.org/html/draft-ietf-manet-dymo-26 [accessed: 2013-11-15].

[46] N. Sivakumar and S. K. Jaiswal, "Comparison of dymo protocol with respect to various quantitative performance metrics," Department of Computer Science, Malardalen University, 2009.

[47] S. K. Bisoyi and S. Sahu, "Performance analysis of dynamic manet on-demand (dymo) routing protocol," Special Issue of IJCCT, vol. 1, no. 2, 2010, p. 3.

[48] C. Perkins, Futurewei, S. Ratliff, Cisco, J. Dowdell, and Cassidian, "Dynamic manet on-demand (AODVv2) routing, draft-ietf-manet-aodvv2-04," Internet-Draft, 2006, URL: https://tools.ietf.org/html/draft-ietf-manet-dymo-04 [accessed: 2013-11-14].

[49] C. Perkins and I. C. Futurewei, "Dynamic manet on-demand (AODVv2) routing," Internet-Draft, 2012, URL: https://tools.ietf.org/html/draft-ietf-manet-dymo-24 [accessed: 2013-11-15].